Outer Leaflet-Packing Defects Promote Poly(ethylene glycol)-Mediated Fusion of Large Unilamellar Vesicles†

JinKeun Lee and Barry R. Lentz*

Department of Biochemistry & Biophysics, University of North Carolina, Chapel Hill, North Carolina 27599-7260

Received September 3, 1996; Revised Manuscript Received November 15, 1996⊗

ABSTRACT: Poly(ethylene glycol)-induced fusion of two different vesicle systems has been examined: dipalmitoylphosphatidylcholine (DPPC) large unilamellar vesicles (LUV) and cardiolipin (CL)/dioleoylphosphatidylcholine (DOPC) (1:10) LUVs. A slight perturbation was established in the outer leaflets of DPPC LUVs by hydrolyzing 0.8% of the outer leaflet lipid with phospholipase A_2 to produce lysophosphatidylcholine and palmitate which were then removed by bovine serum albumin. Similarly, 5 mM Ca^{2+} was added to the external compartment of CL/DOPC LUVs to alter the shape of the CL molecule and thereby create a perturbation in the outer leaflet packing of these vesicles. Contents mixing assays showed that both vesicle systems fused only when the outer leaflets of both contacting vesicles were perturbed as described. Two fluorescent probes (C_6-NBD-PC and TMA-DPH) were used to detect changes in outer leaflet molecular packing between nonfusing and fusing systems. The steady-state fluorescence intensity of C_6-NBD-PC added externally to either fusing system was enhanced relative to that of nonfusing vesicles. Phase-resolved measurements of probe lifetime showed that this was due mainly to enhanced partitioning of probe from a micellar state into fusing versus nonfusing membranes. Similarly, TMA-DPH was found to undergo more rapid motion when incorporated into fusing as opposed to nonfusing vesicles. The effects of deuterium exchange on probe lifetime also indicated that C_6-NBD-PC and TMA-DPH penetrated more deeply into fusing than into nonfusing membranes. These results suggest that the fusogenic perturbations produced in these two very different lipid systems took the form of altered outer leaflet packing. We conclude that, for the two model lipid bilayers examined, small perturbations in lipid packing within contacting bilayer leaflets are necessary and probably sufficient to promote membrane fusion.

Poly(ethylene glycol) (PEG[1])-induced fusion of phospholipid vesicles provides a simple model membrane system that allows molecular level investigations of bilayer events associated with fusion (Lentz, 1994). Briefly, PEG is an effective dehydrating polymer that forces close contact between membranes without directly interacting with them (Arnold *et al*., 1983, 1990). The phenomenology of PEG-mediated vesicle fusion has been described in detail (Lentz, 1994). Briefly, we have shown that close contact between two apposing membranes aggregated by PEG is not sufficient to induce fusion of large unilamellar vesicles (LUV) composed of a single phosphatidylcholine or phosphatidylethanolamine species unless the bilayer is somehow perturbed (Burgess *et al*., 1991; 1992; Lentz *et al*., 1992). Fusion, as documented by a combination of vesicle contents mixing, membrane mixing, and vesicle size change, occurs between two to four vesicles aggregated into small, dehydrated complexes (Massenburg & Lentz, 1993; Wu & Lentz, 1994; Lentz *et al.*, 1996b). Vesicle rupture often occurs at the PEG concentrations needed to produce fusion, but rupture is not necessary for fusion and is thus a separate event associated with the stress created by severe dehydration (Massenburg & Lentz, 1993; Lentz *et al.*, 1996b).

Fusogenic bilayer perturbation includes high bilayer curvature of small unilamellar vesicles (SUV; Suurkuusk *et al*., 1976; Lentz *et al*., 1987; Talbot *et al.*, 1996), acyl chain unsaturation within fusion-prone SUVs (Talbot *et al*., 1996), very small surface mole fractions (0.5 mol %) of lysophosphatidylcholine (LPC; Lentz *et al*., 1992), and imperfect lipid packing caused by manipulation of outer leaflet LPC content (Wu *et al*., 1996). Another view is that fusion is promoted by the appropriate asymmetric location of non-bilayer-forming lipids, *i.e.*, lipids with molecular shapes other than cylindrical (Chernomordik *et al.*, 1995a). In this view, LPC can be either a fusogen if it is located in noncontacting leaflets or a fusion inhibitor if it is located in contacting leaflets. This could provide an alternative explanation for the fusogenicity of LPC-depleted vesicles (Wu *et al*., 1996).

To distinguish between these possibilities, imperfections in the outer leaflet packing of LUVs have been created by generation of packing defects without the addition of amphipathic perturbants such as LPC. In the present paper, two nonfusing vesicle systems, 1,2-dipamitoyl-3-*sn*-phos-

† Supported by USPHS Grant GM32707.

* To whom reprint requests should be directed.

⊗ Abstract published in *Advance ACS Abstracts,* January 1, 1997.

[1] Abbreviations: ANTS, 8-aminonaphthalene-1,3,6-trisulfonic acid disodium salt; BSA, bovine serum albumin; C_6-NBD-PC, 1-palmitoyl-2-[[*N*-(4-nitrobenz-2-oxa-1,3-diazolyl)amino]hexanoyl]phosphatidylcholine; $C_{12}E_8$, dodecyloctaethylene glycol monoether; CL, bovine heart cardiolipin; DOPC, 1,2-dioleoyl-3-*sn*-phosphatidylcholine; DPPC, 1,2-dipalmitoyl-3-*sn*-phosphatidylcholine; DPX, *N,N′-p*-xylenebis(pyridinium bromide); LPC, L-α-lysopalmitoylphosphatidylcholine; LUV, large unilamellar vesicle made by the extrusion technique; PEG, poly(ethylene glycol); PLA_2, phospholipase A_2; POPC, 1-palmitoyl-2-oleoyl-3-*sn*-phosphatidylcholine; SUV, small unilamellar vesicle made by sonication; TES, *N*-[tris(hydroxymethyl)methyl]-2-aminoethanesulfonic acid; TMA-DPH, 1-[4-(trimethylamino)phenyl]-6-phenylhexa-1,3,5-triene.

S0006-2960(96)02233-7 CCC: $14.00

phatidylcholine (DPPC) LUVs and cardiolipin (CL)/1,2-dioleoyl-3-*sn*-phosphatidylcholine (DOPC) (1:10) LUVs, have been modified either by removing 0.4% of the total DPPC from the outer leaflet or by inducing a change in the molecular shape of CL in the outer leaflet by an external addition of 5 mM Ca^{2+}. In both membrane systems, this slight perturbation in the outer leaflet supported PEG-mediated fusion. Furthermore, the perturbation had to be made in both apposing outer leaflets to observe fusion. Disruption of lipid packing in the outer leaflet was characterized using two fluorescent probes, C_6-NBD-PC and TMA-DPH. The results clearly indicate that packing defects in the outer leaflet promote PEG-induced fusion in LUV model membranes.

EXPERIMENTAL PROCEDURES

Materials

Chloroform stock solutions of DPPC, DOPC, bovine heart CL, and 1-palmitoyl-2-[[*N*-(4-nitrobenz-2-oxa-1,3-diazolyl)-amino]hexanoyl]phosphatidylcholine (C_6-NBD-PC) were purchased from Avanti Polar Lipids, Inc. (Birmingham, AL) and used without further purification. The concentrations of phospholipid stocks were determined by phosphate assay (Chen *et al*., 1956). 1-[4-(Trimethylamino)phenyl]-6-phenylhexa-1,3,5-triene (TMA-DPH), the disodium salt of 8-aminonaphthalene-1,3,6-trisulfonic acid (ANTS) and *N*,*N*′-*p*-xylylenebis(pyridinium bromide) (DPX) were purchased from Molecular Probes (Eugene, OR). Carbowax PEG 8000 (molecular weight of 7000−9000) was from Fisher Scientific (Fairlane, NJ) and further purified by a method previously described (Lentz *et al*., 1992). *N*-[Tris-(hydroxymethyl)-methyl]-2-aminoethanesulfonic acid (TES) and bovine serum albumin (BSA) were purchased from Sigma Chemical Co. (St. Louis, MO). Phospholipase A_2 (PLA_2) purified from the venom of *Agkistrodon piscivorus piscvorus* was kindly supplied by professor Rodney Biltonen of the University of Virginia. 1,2-di[^{14}C]palmitoyl-3-*sn*-phosphatidylcholine (lot no. 2708-061) (97%) was purchased from DuPont (Wilmington, DE), and it was added to a DPPC stock solution without further purification. Dodecyloctaethylene glycol monoether ($C_{12}E_8$) was purchased from Calbiochem (La Jolla, CA). Deuterium oxide (99.8% deuterated) was purchased from Aldrich Chemical Co. (Milwaukee, WI). All other reagents were of the highest quality available.

Methods

Vesicle Preparation. Vesicles were prepared by the extrusion method (Hope *et al*., 1985; Mayer *et al*., 1986), as previously described in detail (Lentz *et al*., 1992). DPPC and a mixture of CL and DOPC (1:10) in chloroform were dried under nitrogen. The dried lipids were dissolved in cyclohexane with an aliquot of methanol (about 5 vol %), frozen in dry ice, and dried under high vacuum overnight. The dried lipids were resuspended in an appropriate buffer for about 1 h at a temperature (48 °C for DPPC and 25 °C for CL/DOPC) above the main phase transition. The buffer contained 2 mM TES and 100 mM NaCl (pH 7.4). For the ANTS/DPX contents mixing assay, lipids were suspended in 10 mM TES buffer containing 25 mM ANTS (or 90 mM DPX) and 40 mM NaCl (pH 7.4). For ANTS/DPX contents leakage experiments, the trapped buffer contained 12.5 mM ANTS, 45 mM DPX, 40 mM NaCl, and 10 mM TES (pH 7.4). These buffers were osmotically matched to the 100 mM NaCl buffer. For CL/DOPC vesicles, 0.05 mM EDTA was also included in the buffer to lower the free Ca^{2+} concentration in water. Addition of EDTA prevents both the formation of nonlamellar (hexagonal) CL structures during extrusion and the interaction between inner leaflet CL and free Ca^{2+} in the trapped buffer. The lipid suspensions were then extruded seven times through a 0.1 μm polycarbonate filter (Nucleopore Corp., Pleasanton, CA) above their phase transition under a pressure of 50 psi of argon (Lentz *et al*., 1992). Quasi-elastic light-scattering measurements showed that extruded DPPC vesicles had a mean diameter of 1340 Å while CL/DOPC LUVs had a mean hydrodynamic diameter of 1490 Å. Quasi-elastic light-scattering measurements were carried out by methods described previously (Lentz *et al*., 1992) using a locally built multiangle instrument equipped with a Spectra-Physics Stabilite Model 120 S helium-neon laser (632.8 nm) and a computer-controlled Nicomp 170 autocorrelator (Particle Sizing Systems, Inc., Santa Barbara, CA).

Preparation of Vesicles with Perturbed Outer Leaflets. Packing defects in the outer leaflet of DPPC LUVs were created by partial removal of lipids from the outer leaflet. DPPC LUVs at a concentration of 10 mM were incubated with 100 nM PLA_2 and 1 mM Ca^{2+} at 40 °C for 5 min to hydrolyze a small amount of DPPC from the outer leaflet. Following addition of 2 mM EDTA to quench hydrolysis, vesicles were incubated with 0.5 mM BSA (3.4 wt %) for 20 min at room temperature to remove the reaction products, palmitate and LPC. BSA was separated from the LUVs using a Sepharose CL-4B column (0.8 cm diameter × 19 cm height) at room temperature. The protocol for the PLA_2 reaction was based on that of Burack *et al*. (1995) with modifications for our experimental conditions. The use of BSA to remove LPC and palmitate was adapted from the work by Mohandas *et al*. (1982). More recently, we have demonstrated the use of BSA in removing LPC to create asymmetric vesicles and have shown that BSA concentrations from 1 to 8 wt % and incubation times between 5 and 60 min were all about equally effective in removing ∼0.03 mM LPC from ∼10 mM DPPC LUVs (Wu *et al*., 1996). On the basis of this experience, the conditions we used in this experiment (20 min incubation with 3.4 wt % BSA) are sufficient for removing the LPC and palmitate resulting from hydrolysis of ∼0.032 mM DPPC within a 8 mM LUV sample. Wu *et al*. (1996) also reported that the asymmetry created by LPC removal from outer leaflets remained essentially unchanged for up to 2 h and even remained to some extent after 48 h. In the present paper, all fluorescence measurements and fusion assays were performed within 2 h of BSA treatment.

Packing defects in the outer leaflet of CL/DOPC LUVs were created by a change in the molecular shape of CL from "cylindrical" to "conical" due to addition of 5 mM Ca^{2+} to preformed vesicles (Wilschut *et al.*, 1985; Cullis *et al.*, 1978); control (unperturbed) vesicles were treated with 1 mM EDTA.

ANTS/DPX Contents Mixing and Leakage Measurements. The ANTS/DPX assay has been described previously in detail (Ellens *et al*., 1984; Lentz *et al.*, 1992). CL/DOPC LUVs that contained ANTS, DPX, or a mixture of ANTS and DPX were filtered through a Sephadex G-75 column to

remove the untrapped reagents. A Sepharose CL-4B column was used to remove enzymes as well as untrapped reagents from DPPC LUVs. For the contents mixing assay, ANTS-containing vesicles (0.25 mM) and DPX-containing vesicles (0.25 mM) were mixed with different concentrations of PEG in a 0.4 mL volume. For the contents leakage assay, vesicles (0.5 mM) containing both ANTS and DPX were incubated with PEG in a 0.4 mL volume. For both assays, vesicles were incubated at a temperature (48 °C for DPPC and 25 °C for CL/DOPC LUVs) above their main phase transition for 5 min (enough time for fusion to be completed; Lentz *et al.*, 1992) before dilution to a final volume of 3.5 mL (a final lipid concentration of 0.057 mM), followed by fluorescence intensity measurements. Fluorescence measurements were made on an SLM 48000 MHF spectrofluorometer (SLM Instruments, Rochester, NY) using a focused 450 W xenon lamp (Ushio Inc., Japan) and analyzed to obtain the percent contents mixing and leakage essentially as described previously (Lentz *et al.*, 1992). This analysis corrects for vesicle contents leakage that often occurs in the presence of high PEG concentrations. For the experiment to detect fusion between unperturbed and perturbed DPPC LUVs, perturbed ANTS-containing vesicles and unperturbed DPX-containing vesicles were used in the contents mixing assay; half of a sample of ANTS/DPX-coencapsulated vesicles were perturbed and half left unperturbed for the leakage assay.

Measurements of C_6-NBD-PC and TMA-DPH Fluoresence Properties. A small aliquot (0.06 vol % of vesicle solution) of a stock solution of C_6-NBD-PC (300 nM) in methanol was added to vesicles to create different lipid:probe ratios between 100 and 500. A small aliquot (0.04 vol % of vesicle solution) of a stock solution of TMA-DPH in methanol (700 nM) was added to 0.175 mM vesicles to achieve a lipid:probe ratio of 250. The buffer contained 2 mM TES, 100 mM NaCl, and 1 mM EDTA (pH 7.4) for the unperturbed CL/DOPC LUVs and for both the perturbed and unperturbed DPPC LUVs; or 2 mM TES, 100 mM NaCl, and 5 mM Ca^{2+} (pH 7.4) for the perturbed CL/DOPC LUVs. The vesicle/probe mixture was then vigorously stirred using a micromixer before the fluorescence intensity measurement and continuously stirred at 48 °C for DPPC LUVs and 25 °C for CL/DOPC LUVs using a stirring bar during the measurements. For steady-state measurements of C_6-NBD-PC fluorescence, NBD was excited at a wavelength of 470 nm and its emission intensity was measured through a 2 mm OG-515 filter (Schott Optical Glass, Duryea, PA).

Phase shifts and modulation ratios were collected using an SLM 48000 MHF spectrofluorometer equiped with a Coherent Inova 90 argon-ion laser (Coherent Auburn Group, Auburn, CA). The probes were excited by vertically polarized and modulated light with a wavelength of 488 nm for C_6-NBD-PC and in a region from 351.1 to 363.8 nm of the laser UV multiline for TMA-DPH. The choice of excitation wavelength for C_6-NBD-PC was based on the absorptivity of C_6-NBD-PC in its micellar state, since this probe has a much lower extinction coefficient and quantum yield in the micellar state than in membranes. This optimized the separation of lifetime contributions from the micellar and membrane states. Emission was detected in the L format at an angle of 54.7° from the vertical through a 2 mm OG-515 filter for C_6-NBD-PC and a through a 3 mm KV-450 filter (50% transmission at 450 nm; Schott Optical Glass) for TMA-DPH (Wu & Lentz, 1994). The Dynamic Data Aquisition routine of the SLM 48000 MHF spectroscopy software package was used to collect phase shifts and modulation ratios at 37 frequencies (with a base frequency of 4 MHz) using a 5 s acquisition time, a 300 acquisition average, and a glycogen solution as a zero-lifetime reference. Phase-resolved lifetimes and mole fractions of each lifetime component were estimated using the Global Analysis software package (Globals Unlimited, Urbana, IL). For C_6-NBD-PC, two or three sets of phase shifts and modulation ratios from each sample were collected and analyzed by one-, two-, and three-lifetime-component models with a constraint that lifetimes and mole fractions of each component were linked between these data sets. The best fit was obtained with a three-lifetime-component model with the shortest lifetime component being the same in all membrane samples and in samples containing C_6-NBD-PC only. This component was thus identified as being due to C_6-NBD-PC in the micellar state (see Results). Consequently, the data sets for both perturbed and unperturbed vesicles (four different lipid:probe ratios in both cases) were combined and globally fitted to a three-lifetime-component model with the lifetime of the probe in the micellar state as a global variable and the other two lifetimes and two mole fractions as local variables. The two longer lifetimes of C_6-NBD-PC were averaged and used as a membrane-associated lifetime. The average lifetime (τ_{AV}) was calculated from

$$\tau_{AV} = \frac{\sum_i \alpha_i \tau_i^2}{\sum_i \alpha_i \tau_i}$$

where α_i and τ_i are the mole fraction and lifetime of the *i*th component, respectively (Lakowicz, 1983). For TMA-DPH, three sets of data from each sample were collected and fitted to a two-lifetime-component model (Burgess *et al.*, 1991a) with a constraint that lifetimes and mole fractions of each component were linked between these three data sets.

Fluorescence phase-resolved anisotropy measurements with TMA-DPH were made as described for lifetime measurements except that the emission polarizer in the L format was alternatively set to the vertical and horizontal, to obtain the difference between phase shifts and modulation ratios in these two polarized configurations. Data and error analyses were performed with the Globals Unlimited software package.

Measurements of Deuterium Isotope Sensitivity of the Lifetime. In D_2O, fluorophores with exchangeable protons can undergo a deutrium isotope exchange that causes an increase in quantum yield by reducing nonradiative decay *via* excited-state proton transfer (Stryer, 1966). The ratio of the lifetime of TMA-DPH in D_2O to the lifetime in H_2O depends on the degree of water accessibility to the exchangeable protons (Ho *et al*., 1995; Stubbs *et al*., 1995). Similarly, the lifetime of micellar C_6-NBD-PC in D_2O was 1.6 times that observed in H_2O, indicating that deuterium isotope exchange in C_6-NBD-PC also causes an increase in lifetime and that the ratio of average D_2O and H_2O lifetimes of C_6-NBD-PC can also be used to examine water accessibility to the exchangeable proton of this probe. Since the exchangeable protons are located in the head group region for both

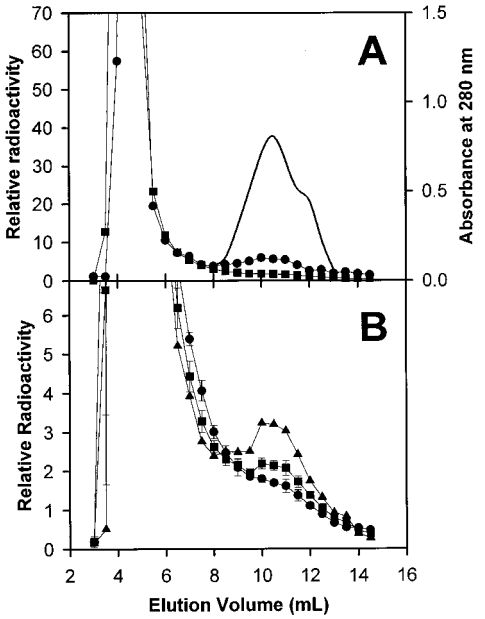

FIGURE 1: Preparation of outer leaflet-perturbed DPPC LUVs. (A) Unperturbed Vesicles. A Sepharose CL-4B column profile (circles) illustrates separation of [^{14}C]DPPC containing DPPC LUVs (early peak) and one or more ^{14}C-containing impurities bound to 0.5 mM BSA (later peak). The line with no symbols shows absorbance at 280 nm and thus the elution of BSA. The elution profile for DPPC LUVs without BSA is also illustrated (squares). DPPC LUVs harvested from the early peak of such a column profile were treated with PLA_2 to obtain asymmetrically perturbed vesicles (see Methods). (B) Perturbed Vesicles. Column profiles are shown for DPPC LUVs incubated with PLA_2 for an incubation time of 0 (control, circles), 5 (squares), and 15 (triangles) min, followed by addition of EDTA and BSA. The elution profiles shown for 0 and 5 min of incubation each represent averages of six sets of data obtained from six separate experiments, and the error bars indicate the standard deviations. Subtraction of the elution profile for the 0 min incubation from that for the 5 min incubation indicated that PLA_2 and BSA treatment removed 0.4 mol % of vesicle total lipids from the outer leaflet.

probes (Chattopadhyay & London, 1987; Stubbs *et al*., 1995), this ratio should reflect hydration or lipid packing in the head group region of the bilayer. Vesicles were prepared in D_2O buffer and then made asymmetric by the procedures described above. All buffers including the column buffer were prepared with D_2O. C_6-NBD-PC was added to the different vesicle systems to produce lipid:probe ratios of 100 and 250 (DPPC) or 125 and 375 (CL/DOPC); TMA-DPH was used at a lipid:probe ratio of 250 for both systems.

RESULTS

Characterization of Outer Leaflet-Perturbed DPPC LUVs. In order to determine the ratio of lipids removed from the outer leaflet to the total lipid content, DPPC LUVs were prepared with a radioactively labeled lipid ([^{14}C]DPPC; 0.16 mol %), and separation of the vesicles from the hydrolysis products was achieved with a Sepharose CL-4B gel filtration column (0.8 cm diameter × 19 cm height). Figure 1A shows the elution profiles of untreated DPPC LUVs containing [^{14}C]-DPPC with (circles) and without (squares) BSA. The radioactivity associated with the BSA-containing peak (~2% of the total) indicates the existence of a slight radioactive impurity (probably labeled palmitic acid) associated with the unperturbed DPPC LUVs. DPPC LUVs treated in this way to remove low-level radioactive impurities were used for

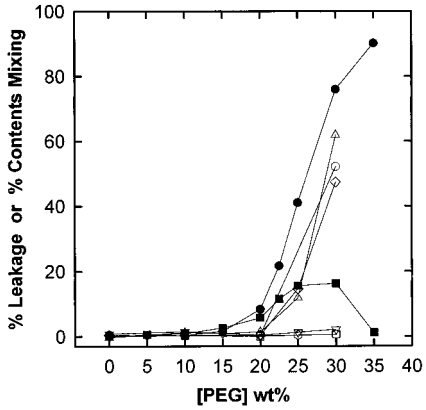

FIGURE 2: Effect of PLA_2 and BSA treatment on DPPC LUV fusion. ANTS/DPX contents leakage (filled circles) and contents mixing (filled squares) for outer leaflet-perturbed DPPC LUVs are shown as a function of PEG concentration. As a control experiment, DPPC LUVs were treated with PLA_2 and BSA in the same way as were the perturbed DPPC LUVs except that the activity of PLA_2 was initially blocked by addition of EDTA. Leakage (open circles) and contents mixing (open squares) were nearly identical to those reported previously for unperturbed DPPC LUVs (Burgess *et al*., 1991). In a second set of experiments, leakage (open triangles) and contents mixing (open inverted triangles) between perturbed and unperturbed DPPC LUVs also indicated no fusion. Finally, the effect of LPC on PEG-mediated contents leakage (open diamonds) and contents mixing (hexagons) of outer leaflet-perturbed DPPC LUVs is shown as a function of PEG concentration. LPC was inserted into the outer leaflet of the perturbed DPPC LUVs by the method of Wu *et al*. (1996), adding 2 mol % LPC in the presence of BSA as a carrier.

preparing asymmetric DPPC LUVs. Figure 1B shows the elution profiles of DPPC LUVs incubated with PLA_2 for times of 0 (control), 5, and 15 min and then treated by addition of EDTA and BSA (see Methods). The ratio of lipid removed from the outer leaflet to the total lipid content was obtained from the ratio of the radioactivity associated with BSA, corrected for a control, to the total radioactivity. The elution profiles for 0 and 5 min of incubation were averaged from six sets of separate experiments to estimate that 0.4% of total lipids was removed from the vesicle in this manner. In this paper, unlabeled vesicles from a 0 min incubation with PLA_2 were used as the unperturbed DPPC LUVs, and unlabeled vesicles from a 5 min incubation were used as the perturbed DPPC LUVs.

PEG-Induced Fusion of Outer Leaflet-Perturbed LUVs. The extents of contents mixing (filled squares) and leakage (filled circles) in outer leaflet-perturbed DPPC LUV preparations are plotted in Figure 2 as function of PEG concentration. A small amount of contents mixing was observed at 15 wt % PEG, without any significant accompanying leakage. Contents mixing was first unambiguously observed at 20 wt % PEG, but it was accompanied by significant leakage. By 35 wt % PEG, no contents mixing was observed, since the trapped contents were largely released by leakage. Contents mixing is a necessary and sufficient indicator of fusion. The control experiment, carried out with DPPC LUVs treated with PLA_2 whose activity was quenched by EDTA and then by BSA (open circles and squares), confirmed our previous report that unperturbed DPPC LUVs do not fuse in the presence of PEG (Burgess *et al*., 1991b) and demonstrated that the fusion observed for perturbed vesicles could not be caused by either PLA_2 or BSA. Leakage of DPPC LUV contents caused by high PEG concentrations has been shown to be due to membrane

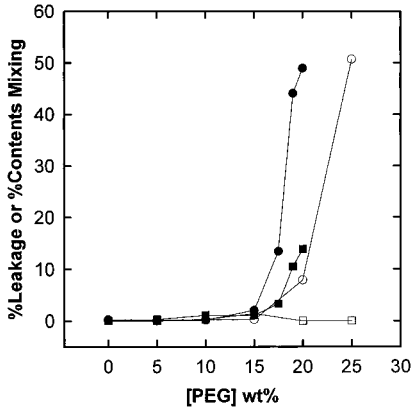

FIGURE 3: Effect of Ca^{2+} on CL/DOPC LUV fusion. ANTS/DPX leakage (circles) and contents mixing (squares) for CL/DOPC (1:10) LUVs in the absence (open symbols) and the presence (filled symbols) of 5 mM Ca^{2+}. The presence of Ca^{2+} in the external aqueous compartment promoted CL/DOPC (1:10) LUV fusion.

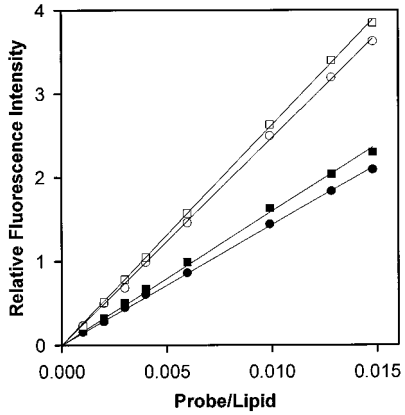

FIGURE 4: Fluorescence intensity of C_6-NBD-PC versus the probe:lipid ratio. Open symbols are for CL/DOPC LUVs at 25 °C in the absence (circles) and the presence (squares) of Ca^{2+}. Filled symbols are for normal DPPC LUVs (circles) and outer leaflet-perturbed DPPC LUVs (squares) at 48 °C. The lines are linear regressions. The intensity has been corrected for background from a reference that was a vesicle solution in the absence of probe.

rupture (Massenburg & Lentz, 1993). The leakage profiles in Figure 2 show that perturbed DPPC LUVs leaked their contents at lower PEG concentrations than did normal DPPC LUVs (equivalent to the control results shown with open symbols in Figure 2), indicating that perturbation of the outer leaflet of DPPC LUVs encouraged not only fusion but also bilayer rupture. However, the observation that PEG-mediated fusion can be observed without vesicle rupture demonstrates that fusion and rupture are different processes (Massenburg & Lentz, 1993; Lentz *et al.*, 1996).

DPPC is a fully saturated lipid with 16 carbon chains. As such, it can be expected to produce a bilayer in which lipids are well packed and that might be expected to be particularly susceptible to the type of packing perturbation produced by the procedures used here. To test whether a bilayer containing lipids more like those found in natural membranes might also be susceptible to packing disruption leading to fusogenicity, we developed a second lipid system containing a mixture of DOPC and CL (10:1 molar ratio) and treated these with Ca^{2+} to produce a change in the shape of the CL molecule from cylindrical to conical (Wilschut *et al.*, 1985; Cullis *et al.*, 1978), a change that would be expected to produce packing disruption. Contents mixing (filled squares) and leakage (filled circles) of the CL/DOPC LUVs treated with 5 mM Ca^{2+} are shown in Figure 3 as a function of PEG concentration. Contents mixing results indicate that Ca^{2+}-treated CL/DOPC LUVs fused at and above 17.5 wt % PEG, while untreated vesicles (open squares) showed no tendency to fuse up to 25 wt % PEG. Leakage profiles showed that the perturbed vesicles (filled circles) ruptured more easily than the unperturbed vesicles (open circles), as was also observed in the DPPC LUV system. In the absence of PEG, Ca^{2+}-treated CL/DOPC LUVs neither fused nor aggregated, as determined by a lack of contents mixing and by the fact that QELS measurements showed that the mean vesicle diameter (1500 Å) was only minimally affected by Ca^{2+} (1670 Å at 23 °C and 1500 Å at 53 °C). Macdonald and Seelig (1987) showed from ^{31}P and ^{2}H NMR spectra that CL/POPC (1:9) bilayers do not experience phase separation over a wide range of Ca^{2+} concentrations. Thus, it is reasonable to conclude that the fusion observed here is promoted not by phase separation or by relaxation of charge repulsion but by the asymmetric perturbation of CL/DOPC vesicles brought about by a Ca^{2+}-induced CL shape change. Evidence of outer leaflet perturbations presented in the next section support this conclusion.

Fluorescence of C_6-NBD-PC to Monitor Perturbation of Vesicle Outer Leaflets. The effects of our manipulations on the surface properties of the membrane outer leaflet were examined using a fluorescent probe, C_6-NBD-PC, which is reported to partition into the upper region of the bilayer (Chattopadhyay & London, 1987) and whose fluorescence intensity has been shown to be sensitive to lipid head group packing (Slater *et al.*, 1994). Figure 4 shows the fluorescence intensity of C_6-NBD-PC, externally added to preformed vesicles, as a function of the probe:lipid ratio in samples to which increasing quantities of probe were added. For each type of LUV, fusing vesicles showed greater fluorescence intensity than nonfusing vesicles, consistent with our earlier observations with asymmetrically perturbed DPPC/LPC LUVs (Wu *et al.*, 1996). C_6-NBD-PC forms micelles above its critical micelle concentraton of 32 nM (Nichols, 1985), which is well below the probe concentrations used in these experiments. Thus, C_6-NBD-PC added to a vesicle solution partitions between the outer membrane leaflet of the vesicles and its micelles (Nichols, 1985; Arvinte *et al.*, 1986). Hence, the fluorescence intensity shown in Figure 4 is the sum of the fluorescence emission from C_6-NBD-PC in the membranes and in the micellar state. However, C_6-NBD-PC in its micellar state shows virtually no fluorescence in the range of concentrations of the probe we have used in this paper due to self-quenching at the high concentration in the micelles (Nichols & Pagano, 1981) and to low absorptivity of micellar C_6-NBD-PC at the excitation wavelength used (470 nm; Lin & Struve, 1991). Therefore, it is reasonable to assume that the fluorescence intensity shown here is a reflection of the fluorescence intensity of C_6-NBD-PC partitioned into the membrane. The fluorescence intensity for DPPC LUVs was much lower than that for CL/DOPC LUVs, at least in part because the measurements were performed at 48 °C for DPPC LUVs and at 25 °C for CL/DOPC LUVs. In both vesicle systems, the fluorescence intensity was greater in vesicles with perturbed outer leaflets (squares in Figure 4). This increase in fluorescence intensity could arise from two effects. One is an increase in the quantum yield of C_6-NBD-PC partitioned

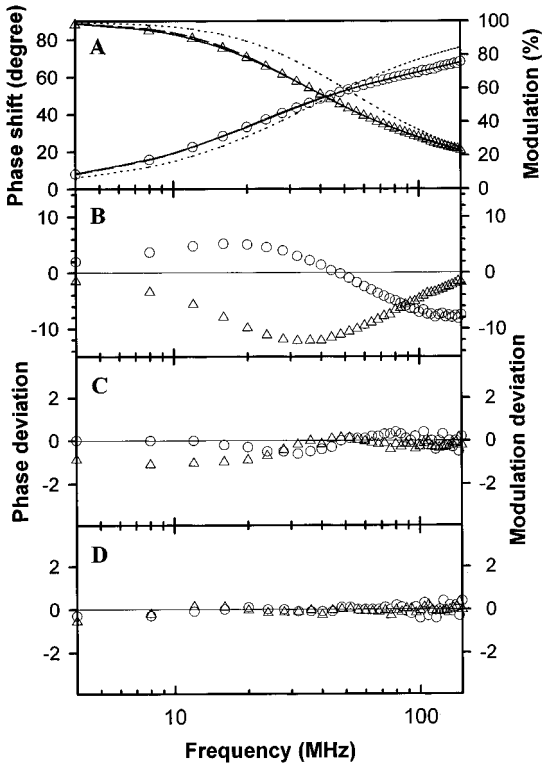

FIGURE 5: Frequency domain fluorescence lifetime determination for C_6-NBD-PC in a CL/DOPC (1:10) LUV suspension (lipid:probe ratio of 250). (A) Phase angle shifts (circles) and modulation ratios (triangles) were fitted to models assuming one (solid), two (dashed), and three (dotted) lifetime components. Residual profiles for the one-, two-, three-component models are shown in frames B, C, and D, respectively, and illustrate that that the best fit was obtained from a three-component analysis. The reduced χ^2 values for one-, two-, and three-component fits were 532.7, 2.02, and 0.87, respectively.

into the membrane. The other is a difference in partitioning of the probe from the micellar to the membrane phase between perturbed and unperturbed vesicles. To distinguish between these possibilities, the lifetime of C_6-NBD-PC in perturbed and unperturbed vesicles was analyzed.

The phase angle shifts and modulation ratios of C_6-NBD-PC at different lipid:probe ratios in LUV suspensions were fitted to one-, two-, and three-lifetime-component models. Examples of the frequency-domain data and the fits thereto are given in Figure 5A for C_6-NBD-PC in CL/DOPC LUVs at a 250:1 lipid:probe ratio. As shown in Figure 5D, the three-component analysis provided an adequate fit. In order to interpret this three-component behavior, the frequency-domain data for C_6-NBD-PC at 25 °C in the absence of vesicles (micellar state) were also collected (Figure 6). Analyses of these data in terms of one- and two-component models were virtually indistinguishable (Figure 6), indicating that C_6-NBD-PC in its micellar state can be well approximated as a single-lifetime species. The single-lifetime parameters for micellar C_6-NBD-PC at 25 and 48 °C as well as examples of the fluorescence decay parameters resulting from a three-component fit to data obtained from vesicle samples are given in Table 1. The lifetime of the shortest lifetime component (τ_3) of C_6-NBD-PC in vesicle suspensions was roughly the same as the single lifetime of C_6-NBD-PC in its micellar state. This was true independent of either the lipid:probe ratio or whether the vesicle system was perturbed or unperturbed. This result suggests that the origin

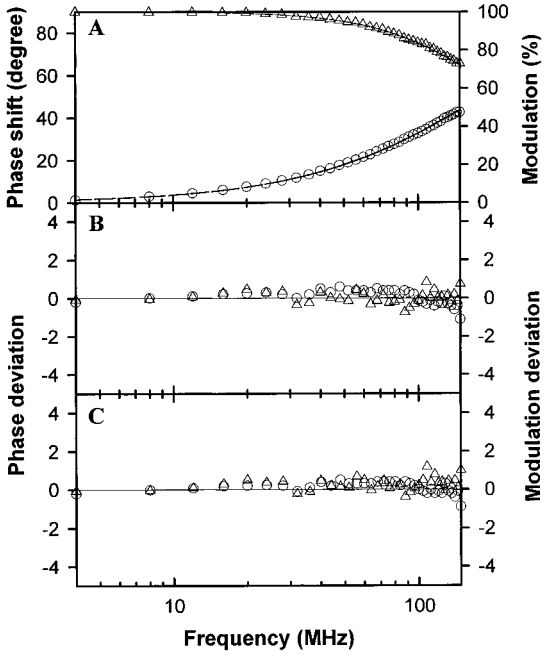

FIGURE 6: Frequency domain fluorescence lifetime determination for C_6-NBD-PC micelles. (A) Phase angle shifts (circles) and modulation ratios (triangles) were fitted to models assuming one (solid) and two (dashed) lifetime components. Residual profiles are shown in frames B (one-component fit) and C (two-component fit). The two-component fit showed little improvement compared to a one-component model. The reduced χ^2 values for one- and two-component fitting were 2.07 and 1.71, respectively.

of the shortest lifetime component in the vesicle system is micellar-state C_6-NBD-PC and that the two longer lifetime components (τ_1 and τ_2) result from C_6-NBD-PC partitioned into the membrane. The reason for the need for two lifetimes to describe membrane-associated probes is not certain and is beyond the focus of this paper, although it may be related to the coexistence of monomeric and cluster populations, as has been proposed for NBD-PE in membranes (Arvinte *et al*., 1986).

To estimate the effect of the perturbation on the fluorescence properties of C_6-NBD-PC partitioned into the membrane, the frequency-domain data for both perturbed and unperturbed vesicles with different lipid:probe ratios were combined and globally analyzed using a three-lifetime-component model. In this analysis, the shortest lifetime component was fixed as that for micellar C_6-NBD-PC, independent of either the lipid:probe ratio or the perturbation. The lifetimes of the other two components and their intensity fractions were adjusted to fit the data for different lipid:probe ratios for either the perturbed or unperturbed vesicles. The average lifetimes of these two membrane-associated lifetime components were taken to reflect the local environment of C_6-NBD-PC partitioned into either pertubed or unperturbed membranes, and the sum of the mole fractions of these two components was taken to reflect the partitioning of C_6-NBD-PC into the membrane. These quantities are plotted against the lipid:probe ratio in Figures 7 and 8 for DPPC LUVs and CL/DOPC LUVs, respectively. The average lifetime of the probe partitioned into DPPC LUVs (Figure 7A) was in the range of 5.52−5.55, largely independent of the lipid:probe ratio, for the perturbed vesicles (squares) and in the range of 5.44−5.51, showing a slight increase with the lipid:probe ratio for the unperturbed vesicles (circles). The fact that the average lifetime of the probe in the perturbed vesicles was

Table 1: Lifetime Components[a] for C_6-NBD-PC in Phosphatidylcholine LUVs

LUVs	lipid:probe	τ_1[b]	α_1[c]	τ_2	α_2	τ_3	α_3	χ^{2}[d]
CL/DOPC	0 (25 °C)	–	–	–	–	1.029	1.000	2.210
	100	7.925	0.175	4.388	0.362	0.916	0.463	1.216
	175	8.314	0.145	4.597	0.396	0.959	0.459	0.916
	250	8.453	0.159	4.677	0.403	0.974	0.438	1.174
	325	8.436	0.173	4.611	0.398	0.981	0.429	0.993
CL/DOPC + 5mM Ca^{2+}	250	8.724	0.163	4.835	0.410	1.041	0.427	1.094
DPPC	0 (48 °C)	–	–	–	–	0.842	1.000	2.485
	250	6.694	0.168	4.689	0.302	0.810	0.530	1.891
DPPC (perturbed)	250	6.791	0.204	4.843	0.290	0.817	0.506	1.241

[a] Lifetime analysis was carried out by Global Analysis software from Globals Unlimited using two or three data sets for each sample. [b] τ_i is the fluorescence lifetime (nanoseconds) of the *i*th component. [c] α_i is the mole fraction of the *i*th component. [d] χ^2 is the reduced χ^2 and represents the goodness of the fit.

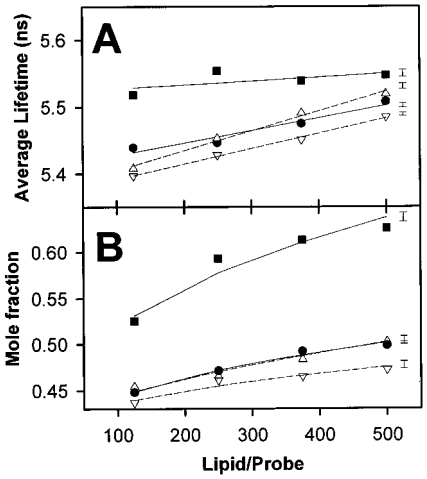

FIGURE 7: Lifetimes and mole fractions of C_6-NBD-PC partitioned into DPPC LUV and asymmetric DPPC LUV suspensions. Comparison between DPPC LUVs (filled circles) and DPPC LUVs perturbed by PLA_2 treatment (filled squares) showed increases in both (A) lifetimes and (B) mole fractions of membrane-associated probe with an increasing lipid:probe ratio. Comparison between DPPC LUVs (triangles) and perturbed DPPC LUVs treated with LPC (inverted triangles) is also presented. Each comparison was made by analyzing the data from both perturbed and unperturbed systems globally. The two frames show (A) average lifetimes of the probe partitioned into the membrane and (B) the sum of the mole fractions of the two longer lifetime components, which reflects the mole fraction of probe partitioned to the membrane. The lines are least-squares fits: linear for lifetimes (A) and quadratic for mole fractions (B). The error bars indicate the root mean square variances for these fits.

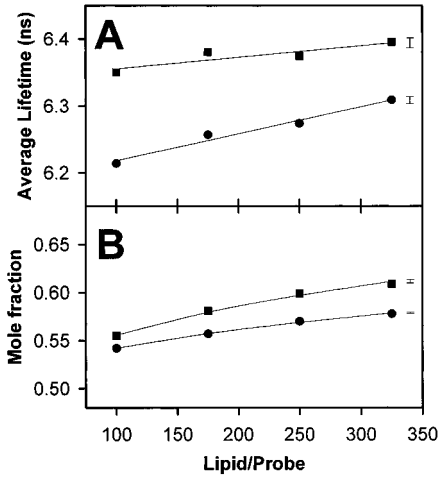

FIGURE 8: Lifetimes and mole fractions of C_6-NBD-PC partitioned in DPPC LUV (circles) and outer leaflet-perturbed DPPC LUV (squares) suspensions. Frame A shows the average lifetime of the probe partitioned to the membrane phase, while frame B shows the mole fraction of probe associated with the membrane, as defined in Figure 7. The lines are least-squares fits: linear for lifetimes (A) and quadratic for partitioning (B). The error bars indicate the root mean square variances of the fits.

longer than that in the unperturbed vesicles indicates that the local environment of the probe was either more hydrophobic or less dynamic in the perturbed membranes than in the unperturbed membranes. The mole fraction of the probe partitioned into DPPC LUVs (Figure 7B) increased gradually with an increasing lipid:probe ratio from 0.53 to 0.63 for the perturbed vesicle (filled squares) and from 0.45 to 0.50 for the unperturbed vesicles (filled circles). At all lipid:probe ratios, the mole fraction of the probe in the membranes was substantially increased (17−26%) by perturbation of DPPC LUVs. For CL/DOPC LUVs, the average lifetime of the membrane-associated probe (Figure 8A) was in the range of 6.35−6.40 for perturbed vesicles (squares) and of 6.21−6.31 for unperturbed vesicles (circles). Thus, as for DPPC LUVs, the lifetime of the probe in perturbed vesicles was longer than that in unperturbed vesicles. The lifetime of the probe in the perturbed vesicles was nearly independent of the lipid:probe ratio, while that in unperturbed vesicles increased with the lipid:probe ratio. The mole fraction of the probe partitioned from micelles to CL/DOPC LUVs (Figure 8B) was in the range of 0.56−0.61 for perturbed vesicles (squares) and 0.54−0.58 for unperturbed vesicle (circles). Thus, a smaller increase (4−5%) in C_6-NBD-PC partitioning into pertubed than into unpertubed vesicles was observed for CL/DOPC versus DPPC LUVs. Despite this quantitative difference, however, the qualitative effect of outer leaflet perturbation on C_6-NBD-PC was the same for both types of vesicle systems: enhanced probe partitioning into the membrane and increased quantum yield or fluorescence lifetime of the membrane-associated probe.

Outer Leaflet Perturbation Is Necessary for Fusogenicity. The importance of outer leaflet perturbation to fusion between PEG-aggregated vesicles is illustrated by two other experiments summarized in Figure 2. First, we tested whether the outer leaflets of both members of an aggregated pair of vesicles had to be perturbed in order to obtain fusion. As is demonstrated in Figure 2, the contents mixing profile (open inverted triangles) of a mixture of perturbed and unperturbed DPPC LUVs showed no sign of fusion up to 30 wt % PEG; the leakage profile of this vesicle system (open triangles) was similar to that of normal DPPC LUVs (Burgess *et al.*, 1991b). This result indicates that both apposing outer leaflets must be perturbed to promote PEG-mediated fusion of DPPC LUVs. Second, we showed that the effect of outer

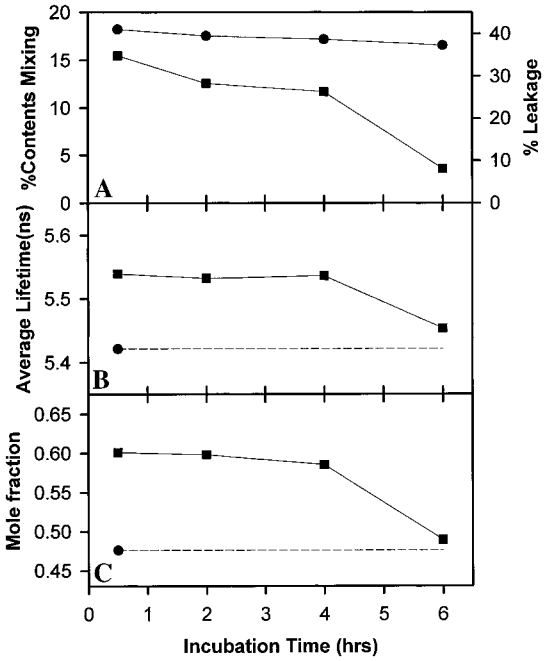

FIGURE 9: Time dependence of the fusion and outer leaflet perturbation of perturbed DPPC LUVs. (A) ANTS/DPX leakage (circles) and contents mixing (squares) were monitored 5 min after mixing with 25% PEG. (B) Lifetimes and (C) mole fractions of C_6-NBD-PC partitioned in DPPC LUVs (circles) and the outer leaflet-perturbed DPPC LUVs (squares) with a lipid:probe ratio of 250. The incubation time is the time between asymmetric vesicle preparation and fluorescence measurements. Incubation and fluorescence measurements were carried out at 48 °C. All the measurements presented in this paper, except those presented in this figure, were made within 2 h of preparation of the perturbed vesicles.

leaflet perturbation could be blocked by addition of LPC to the outer leaflet, as indicated by the lack of contents mixing between LPC-treated vesicles (hexagons in Figure 2). A similar effect of LPC has been reported for planar lipid bilayer systems (Chernomordik *et al.*, 1995a) and for DPPC LUVs asymmetrical in LPC content (Wu *et al.*, 1996). Because the perturbed vesicles reported here were prepared without use of LPC, there is little chance that their fusogenicity is due to LPC located on their inner leaflets, a possibility that could not be ruled out in the work of Wu *et al.* (1996). In addition to blocking fusion, externally added LPC reversed the perturbation of DPPC LUV outer leaflets caused by PLA_2 treatment (inverted triangles in Figure 7). The ability of externally added LPC to reverse outer leaflet perturbation and to block fusion suggests strongly that the root cause of fusogenicity is the perturbation caused by removal of a small amount of lipid mass from the outer leaflet of DPPC vesicles.

Further evidence that outer leaflet perturbation is closely related to fusogenicity is shown in Figure 9. The asymmetrically perturbed DPPC LUVs created here maintained their ability to fuse for nearly 4 h but quickly lost this in the next 1−2 h. The loss of outer leaflet perturbation monitored by the fluorescence of C_6-NBD-PC (Figure 9A,B) paralleled the loss of fusogenicity of these vesicles as measured by the contents mixing assay (Figure 9C). This relief of asymmetric perturbation is probably due to slow transmembrane redistribution, eventually resulting in well-packed outer leaflets similar to those of normal DPPC LUVs. The parallel behavior of outer leaflet perturbation and fusogenicity is strong evidence that the fusion of perturbed DPPC LUVs was due to poor packing of the outer leaflet.

Fluorescence of TMA-DPH to Monitor Perturbation of Vesicle Outer Leaflets. In order to define more precisely the effects of the outer leaflet perturbations we have introduced, we examined the fluorescence properties of TMA-DPH, a membrane probe that we have shown to be sensitive to fusion-inducing perturbations (Lentz *et al.*, 1996). We examined first the excited-state lifetime of this probe. Phase angle shifts and modulation ratios for TMA-DPH in LUV suspensions (lipid:probe ratio of 250) were well fit by a two-lifetime model, with the results collected in Table 2. The average lifetime of the probe in perturbed CL/DOPC LUVs was slightly greater than that in unperturbed vesicles. However, the average lifetime of TMA-DPH in perturbed DPPC LUVs was not different from that in unperturbed vesicles. This result could indicate that the environment of the DPH fluorophore was similar in perturbed and unperturbed vesicles or that there were compensating effects of perturbation on the lifetime of TMA-DPH fluorescence. We will return to this point.

To examine in more detail the effects of outer leaflet perturbation on TMA-DPH, we monitored the differences in phase shifts and modulation ratios as detected through vertically and horizontally oriented polarizers. This method provides information about the dynamics of probe motion (Lakowicz *et al.*, 1993). Several models were tested to describe the data (a single or double lifetime coupled with hindered rotation in a cone or a P2−P4 orientational potential motional model), and as reported previously (Lentz *et al.*, 1996), the simplest physically reasonable model to describe adequately the data was one assuming two lifetimes and simple hindered rotation in a cone (Kinosita & Ikegami, 1984). The parameters obtained from such a description of the data are summarized in Table 2. As can be seen from the tabulated motional parameters, perturbation of the outer leaflet by either method (PLA_2 or Ca^{2+}) resulted in no change in the extent of probe motion (related to the limiting anisotropy, r_∞) but did lead to an increase in the rate of probe rotation (decrease in the rotational correlation time, ϕ). Since the thermal motion of TMA-DPH increased in membranes prone to fusion, it is hard to understand why the lifetime of this probe did not decrease in perturbed membranes. Indeed, the lifetime of C_6-NBD-PC even increased in perturbed membranes (Figures 7 and 8). In an attempt to understand the behavior of the probe lifetime in perturbed membranes, we asked whether these probes might be located differently in unperturbed versus perturbed membranes.

Deuterium Isotope Effects on Fluorescence Decay. In order to examine the possibility of outer leaflet perturbation altering probe location, deuterium isotope replacememt experiments were carried out. Fluorophores having an exchangeable hydrogen, such as TMA-DPH and C_6-NBD-PC, experience H_2O-mediated quenching that is reduced in the presence of D_2O (Stryer, 1966). Thus, an increase in the fluorescent lifetime in the presence of D_2O is evidence of exposure of a probe to water (Ho *et al.*, 1995; Stubbs *et al.*, 1995). The ratio of the average probe lifetime in D_2O to that in H_2O ($\tau_{AV}^{D_2O}/\tau_{AV}^{H_2O}$) for TMA-DPH (Table 2) and for C_6-NBD-PC (Table 3) was determined. The $\tau_{AV}^{D_2O}/\tau_{AV}^{H_2O}$ ratio for TMA-DPH in the unperturbed vesicles was fairly high (1.20 for CL/DOPC and 1.15 for DPPC), while the ratio dropped significantly for perturbed vesicles (1.07

Table 2: Lifetime Components[a] for TMA-DPH and Analysis of Its Motion in Phosphatidylcholine LUVs

LUVs	τ_1[b]	α_1	τ_2	χ^2	τ_{AV}	r_∞[c]	ϕ (ns)	$\tau_{AV}^{D_2O}/\tau_{AV}^{H_2O}$ [d]
CL/DOPC (1:10)[e]	3.52	0.50	0.95	1.02	2.98 ± 0.039	0.097 ± 0.007	2.664 ± 0.127	1.20 ± 0.033
CL/DOPC (1:10) + 5 mM Ca^{2+} [f]	3.53	0.53	0.94	0.97	3.04 ± 0.033	0.099 ± 0.006	2.283 ± 0.093	1.07 ± 0.029
DPPC[e]	3.58	0.54	0.71	0.98	3.16 ± 0.037	0.107 ± 0.002	1.363 ± 0.019	1.15 ± 0.030
DPPC (PLA_2-treated)[f]	3.59	0.55	0.75	1.15	3.17 ± 0.044	0.111 ± 0.002	1.071 ± 0.016	1.05 ± 0.029

[a] For each sample, three data sets were collected and fitted to a two-component model using Global Analysis software from Globals Unlimited, where α_i and τ_i are as defined in Table 1. Lifetime measurements were carried out for samples using both H_2O and D_2O buffers, and their average lifetime ratio ($\tau_{AV}^{D_2O}/\tau_{AV}^{H_2O}$) was used to guage exposure to water. [b] Lifetime parameters shown here are for samples using H_2O. The uncertainty of the average lifetime was approximated asymtotically (Bevington, 1969) using the uncertainty of each lifetime component obtained from Globals error analysis with confidence of one standard deviation. [c] The limiting fluorescence anisotropy (r_∞) and rotational correlation time (ϕ) were obtained using Globals assuming the probe as a free rotator in an orientational potential represented by a hard cone. Errors represent one standard deviation in the parameter values. [d] Errors on the average lifetime ratios were calculated using the uncertainties of average lifetime in D_2O and H_2O. [e] Unperturbed vesicles. [f] Perturbed vesicles.

Table 3: Average Lifetimes[a] of Membrane-Associated C_6-NBD-PC in H_2O and D_2O Buffers

LUVs	$\tau_{AV}^{D_2O}$	$\alpha_{AV}^{D_2O}$	$\tau_{AV}^{D_2O}/\tau_{AV}^{H_2O}$
CL/DOPC (1:10) (375)[b]	7.12 ± 0.043	0.52 ± 0.012	1.15 ± 0.039
CL/DOPC (1:10) (375) + 5 mM Ca^{2+} [c]	6.66 ± 0.051	0.54 ± 0.013	1.05 ± 0.030
CL/DOPC (1:10) (125)[b]	7.18 ± 0.039	0.56 ± 0.012	1.14 ± 0.027
CL/DOPC (1:10) (125) + 5 mM Ca^{2+} [c]	6.64 ± 0.044	0.61 ± 0.014	1.04 ± 0.034
DPPC (250)[b]	6.14 ± 0.047	0.44 ± 0.011	1.13 ± 0.031
DPPC (250) (asymmetric)[c]	5.72 ± 0.052	0.55 ± 0.009	1.04 ± 0.040
DPPC (100)[b]	6.20 ± 0.049	0.47 ± 0.010	1.13 ± 0.027
DPPC (100) (asymmetric)[c]	5.75 ± 0.045	0.60 ± 0.009	1.04 ± 0.032

[a] Fluoresecence lifetime analyses were performed as described in Table 1 with average values calculated as described in Methods from components 1 and 2 listed in Table 1. Errors were calculated as described in Table 2. [b] Unperturbed vesicles. [c] Perturbed vesicles.

for CL/DOPC and 1.05 for DPPC). Similar larger values of the $\tau_{AV}^{D_2O}/\tau_{AV}^{H_2O}$ ratio for C_6-NBD-PC were observed in unperturbed (1.13−1.15) than in perturbed (1.04−1.05) vesicles. These results indicate that both these probes experienced an environment containing less water in perturbed than in unperturbed vesicles. This is surprising, since the manipulations performed on these vesicles produced outer leaflets with more space to accommodate the C_6-NBD-PC probe (Figures 7B and 8B) and to allow more rapid TMA-DPH motion (Table 2). We anticipate, therefore, that they should accommodate the entry of more water into the upper regions of the bilayer. The explanation that we offer for this seeming anomaly is that the perturbations in the outer leaflet probably allowed deeper penetration of the probes into the more hydrophobic regions of the membrane. This would explain why the lifetime of the C_6-NBD-PC probe increased in perturbed membranes despite the fact that the opportunities for thermal quenching should have increased (on the basis of the increased rate of motion of TMA-DPH).

DISCUSSION

Manipulations Produce Packing Defects in Outer Leaflets. In the present paper, we have prepared LUVs asymmetrically perturbed in their outer leaflets either by removal of a small amount of PLA_2-hydrolyzed lipid or by inducing shape changes in CL with Ca^{2+}. That these perturbations produced packing defects was demonstrated by enhanced partitioning of C_6-NBD-PC into the perturbed vesicles as well as by an increased rate of thermal motion of TMA-DPH in perturbed membranes. These packing defects allow for deeper penetration of both fluorescent probes into the bilayer and, of greatest interest to us, appear to facilitate fusion of vesicles aggregated by PEG.

A similar proposal of a pertubed outer leaflet favoring fusion has been made in the case of DPPC/LPC LUVs with a small amount of LPC removed from their outer leaflets. This proposal was based in part on the greater fluorescence intensity of C_6-NBD-PC in these fusing vesicles (Wu *et al*., 1996). Slater *et al*. (1994) have also suggested that the intensity of C_6-NBD-PC fluorescence is sensitive to lipid head group spacing or hydration. We suggest here that a problem with such a simple interpretation is that changes in fluorescence intensity can reflect a range of changes in probe behavior in different membranes: quantum yield, partitioning into the membrane, location in the membrane, and aggregation state in the membrane, all of which could be caused by the type of perturbation we introduced here. Phase-resolved measurement of the fluorescence lifetime of C_6-NBD-PC showed an increase in both the average lifetime and the partitioning of the probe into the outer leaflet for both types of fusing as opposed to nonfusing vesicles. The increased probe lifetime was unexpected in light of what we expect to be increased water partitioning into perturbed outer leaflets. Although the average location of the NBD fluorophore of C_6-NBD-PC has been reported to be at the glycerol backbone region (Chattopadhyay & London, 1987), it seems to alter its position toward the upper acyl chain region in response to the perturbations we introduced. This scenario has been clearly proved by a decrease in our measurements of the $\tau_{AV}^{D_2O}/\tau_{AV}^{H_2O}$ ratios. Therefore, the increase in the average lifetime of C_6-NBD-PC partitioned into membranes would be a reflection of deeper penetration of the probe into fusing than into nonfusing vesicles.

The lifetime of TMA-DPH was insensitive to whether this probe was incorporated into nonfusing or fusing vesicles, although a decreased $\tau_{AV}^{D_2O}/\tau_{AV}^{H_2O}$ ratio indicates that the probe partitions more deeply into fusing than into nonfusing vesicles. The lifetime of DPH is sensitive to the dielectric constant gradient along the membrane normal (Fiorini *et al*., 1987). Thus, the lifetime decrease that should accompany

greater rotational mobility of TMA-DPH or the expected accompanying increased water penetration in fusing versus nonfusing vesicles may have counteracted the lifetime increase expected to accompany enhanced penetration of the probe.

Packing defects are also indicated by increased C_6-NBD-PC partitioning into perturbed outer leaflets. For DPPC LUVs, the large increase in partitioning into the membrane suggests that removal of 0.8 mol % lipids from outer leaflets created significant packing defects. For CL/DOPC LUVs, the increase in partitioning was smaller but the increase in the average lifetime was larger than that shown in DPPC LUVs. Apparently, the perturbation produced by a change of CL shape from cylindrical to conical did not produce as severe a packing defect in the unsaturated DOPC bilayer as did removal of a small amount of lipid from the saturated and well-ordered DPPC bilayer.

Further evidence for outer leaflet-packing defects introduced into the model membranes studied here is provided by the motion of TMA-DPH. This probe can be added from the aqueous medium directly to perturbed vesicles and probably probes the C_1-C_{10} upper regions of the bilayer (Ho *et al*., 1995). Since it migrates very slowly across the bilayer (Lentz *et al.*, 1996), it measures only the outer leaflet altered by our manipulations. Analysis of differential polarized phase shifts and modulation ratios in terms of a model assuming hindered rotation in a cone (Kinosita & Ikegami, 1984) clearly suggests more rapid thermal motions in the upper region of bilayers that can fuse in the presence of PEG as compared to those that cannot. This is consistent with our finding that DPPC LUVs rendered fusogenic by small amounts of amphipathic compounds such as LPC or platelet-activating factor were somehow structually altered in the interface or upper regions of the bilayer (Lentz *et al.*, 1996). The present study provides clear evidence of enhanced thermal motions and decreased packing density in this region of membranes that can be induced to fuse in the presence of PEG. Both these properties would be consistent with enhanced water penetration into and increased surface tension of fusogenic bilayer leaflets, although we can offer no direct evidence for this due to the fact that probes purported to measure water penetration apparently adjust their vertical position in the bilayer to reduce what would be thermodynamically unfavorable contact with water.

Packing Defects in LUV Outer Leaflets Are Necessary and Probably Sufficient To Promote PEG-Induced Fusion. It has been proposed that the shape of the lipid components (*e.g.*, cone or inverted cone. negative or positive curvature, inverted hexagonal phase-forming or hexagonal phase-forming) plays an important role in promoting or inhibiting membrane fusion. Depending on the location and shape of the lipid component, it may stabilize or destabilize either the fusion intermediate or pore formation (Chernomordik *et al*., 1995b). For example, a hexagonal phase-forming species such as LPC would inhibit stalk formation and thus inhibit fusion when incorporated into the outer leaflet of a fusing system (Figure 2), while it should favor pore formation and thus promote fusion when inserted into the inner leaflet (Chernomordik *et al*., 1995a). We refer to this as the *outer/inner leaflet intrinsic curvature hypothesis*. We have recently demonstrated that DPPC/LPC LUVs fused when LPC in the outer leaflet was partially removed to produce asymmetric vesicles with a small excess of LPC in the inner leaflet (Wu *et al.*, 1996). According to the leaflet intrinsic curvature model, the observation of Wu *et al.* on the fusion of DPPC LUVs with asymmetrically distributed LPC can be viewed as a reflection of competition between inhibition of stalk formation by LPC in the outer leaflet and promotion of pore formation by LPC in the inner leaflet. However, we interpreted these observations and the correlation of C_6-NBD-PC fluorescence with vesicle fusogenicity to mean that packing defects in the outer leaflet may play a more important role than the shape of LPC in promoting fusion (Wu *et al*., 1996). We refer to this as the *outer leaflet-packing stress hypothesis*. It was not possible to distinguish between these two models. In the present paper, we demonstrate that perturbation of outer leaflet packing without any alteration in the inner leaflet of nonfusing systems is sufficient to promote fusion independent of the shape of lipid components (cylindrical DPPC or conical CL). Furthermore, we have shown that both apposing outer leaflets must be perturbed to promote fusion (Figure 2). Most significantly, outer leaflet packing was restored to normal (Figure 7) and fusion was inhibited (Figure 2) when LPC was added to asymmetrically perturbed DPPC LUVs. These results clearly demonstrate that, in the case of DPPC LUVs, outer leaflet packing disruption is necessary to cause fusion, and there is no need to invoke lipid shape arguments to explain our observations or those of Wu *et al.* (1996).

The promotion of fusion of CL/DOPC LUVs by CL shape changes could also fit the intrinsic curvature hypothesis proposed by Chernomordik *et al.* (1995b), since the cone shape of CL in the presence of Ca^{2+} would favor stalk formation and promote fusion. However, it has been shown that the incorporation of arachidonic acid (a cone-shaped lipid) into the outer leaflet of a fusing system caused no observable effect on fusion (Chernomordik *et al*., 1995a). In addition, DPPC LUVs containing diacylglycerols, which have a cone shape (Gruner, 1985) like CL in the presence of Ca^{2+}, showed no sign of hemifusion (Lentz *et al*., 1992). Thus, the presence of conical lipids in the bilayer may not be sufficient to promote fusion. Rather than lipids of a particular molecular shape, our results indicate that the fundamental requirement for fusion is some type of manipulation that results in contacting membrane surfaces having a high-free energy interface between the hydrophobic membrane interior and the water phase. *Altering* the shape of outer leaflet lipids (*i.e.*, changing the intrinsic outer leaflet curvature) appears to be one way to accomplish this; removing a small amount of mass from this leaflet appears to be another way to produce such a high-free energy interface. Within the context of the stalk−pore model (Kozlov *et al.*, 1989), such contacting high-free energy surfaces would have a high probability of relaxing to a stalk intermediate. This intermediate can presumably decay by some unknown mechanism toward the fused state.

Finally, we note that our results do not address the second half of the outer/inner leaflet intrinsic curvature hypothesis, namely the importance of positive intrinsic curvature of the inner leaflet. Since we have made no effort to perturb membrane inner leaflets in this study, it would seem that inner leaflet perturbation is not necessary for fusion, although it may enhance fusion. To resolve this point, studies of inner laflet-perturbed vesicles will be needed. Until these are performed, we must conclude that outer leaflet perturbation

is necessary and probably sufficient for fusion of contacting bilayers.

REFERENCES

Arnold, K., Pratch, L., & Gawrisch, K. (1983) *Biochim. Biophys. Acta 728*, 121−128.

Arnold, K., Zschoernig, O., Bacthel, D., & Herold, W. (1990) *Biochim. Biophys. Acta 1022*, 303−310.

Arvinte, T., Cudd, A., & Hildenbrand, K. (1986) *Biochim. Biophys. Acta 860*, 215−228.

Bevington, P. R. (1969) *Data Reduction and Error Analysis for the Physical Sciences*, pp 56−65, McGraw-Hill, New York.

Burack, W. R., Gadd, M. E., & Biltonen, R. L. (1995) *Biochemistry 34*, 14819−14828.

Burgess, S. W., Wu, J. R., Swift, K., & Lentz, B. R. (1991a) *J. Fluoresc. 1*, 105−112.

Burgess, S. W., Massenburg, D., Yates, J., & Lentz, B. R. (1991b) *Biochemistry 30*, 4193−4200.

Chattopadhyay, A., & London, E. (1987) *Biochemistry 26*, 39−45.

Chen, P. S., Jr., Toribara, T. Y., & Warner, H. (1956) *Anal. Chem. 28*, 1756−1758.

Chernomordik, L., Chanturiya, A., Green, J., & Zimmerberg, J. (1995a) *Biophys. J. 69*, 922−929.

Chernomordik, L., Kozlov, M. M., & Zimmerberg, J. (1995b) *J. Membr. Biol. 146*, 1−14.

Cullis, P. R., Verkleij, A. J., & Ververgaert, P. H. J. T. (1978) *Biochim. Biophys. Acta 513*, 11−20.

Ellens, H., Bentz, J., & Szoka, F. C. (1984) *Biochemistry 23*, 1532−1538.

Fiorini, R., Valentino, M., Wang, S., Glaser, M., & Gratton, E. (1987) *Biochemistry 26*, 3864−3870.

Ho, C., Slater, S. J., & Stubbs, C. D. (1995) *Biochemistry 34*, 6188−6195.

Hope, M. J., Bally, M. B., Webb, G., & Cullis, P. R. (1985) *Biochim. Biophys. Acta 812*, 55−65.

Kinosita, K., & Ikegami, A. (1984) *Biochim. Biophys. Acta 769*, 523−527.

Kozlov, M. M., Leikin, S. L., Chernomordik, L. V., Markin, V. S., & Chizmedzhev, Y. A. (1989) *Eur. Biophys. J. 17*, 121−129.

Lakowicz, J. R. (1983) *Principles of Fluorescence Spectroscopy*, Plenum Press, New York.

Lakowicz, J. R., Cherek, H., Kusba, J., Gryczynski, I., & Johnson, M. L. (1993) *J. Fluoresc. 3*, 103−116.

Lentz, B. R. (1994) *Chem. Phys. Lipids 73*, 91−106.

Lentz, B. R., Carpenter, T. J., & Alford, D. R. (1987) *Biochemistry 26*, 5389−5397.

Lentz, B. R., McIntyre, G. F., Parks, D. J., Yates, J. C., & Massenburg, D. (1992) *Biochemistry 31*, 2643−2653.

Lentz, B. R., Wu, J. R., Zheng, L.-X., & Převrátil, J. (1996a) *Biophys. J.* (in press).

Lentz, B. R., Talbot, W., Lee, J. K., & Zheng, L.-X. (1996b) *Biochemistry* (submitted for publication).

Lin, S., & Struve, W. S. (1991) *Photochem. Photobiol. 54*, 361−365.

Macdonald, P. M., & Seelig, J. (1987) *Biochemistry 26*, 6292−6298.

Massenburg, D., & Lentz, B. R. (1993) *Biochemistry 32*, 9172−9180.

Mayer, L. D., Hope, M. J., & Cullis, P. R. (1986) *Biochim. Biophys. Acta 856*, 161−168.

Mohandas, N., Wyatt, J., Mel, S. F., Rossi, M. E., & Shohet, S. B. (1982) *J. Biol. Chem. 257*, 6537−6543.

Nichols, J. W. (1985) *Biochemistry 24*, 6390−6398.

Nichols, J. W., & Pagano, R. E. (1981) *Biochemistry 20*, 2783−2789.

Slater, S. J., Kelly, M. B., Taddeo, F. J., Ho, C., Rubin, E., & Stubbs, C. D. (1994) *J. Biol. Chem. 269*, 4866−4871.

Stryer, L. (1966) *J. Am. Chem. Soc. 88*, 5708−5712.

Stubbs, C. D., Ho, C., & Slater, S. J. (1995) *J. Fluoresc. 5*, 19−28.

Suurkuusk, J., Lentz, B. R., Barenholtz, R. L., Biltonen, R. L., & Thompson, T. E. (1976) *Biochemistry 15*, 1393−1401.

Talbot, W. A., Zheng, L.-X., & Lentz, B. R. (1996) *Biochemistry* (submitted for publication).

Wilschut, J., Nir, S., Scholma, J., & Hoekstra, D. (1985) *Biochemistry 24*, 4630−4636.

Wu, H., Zheng, L.-X., & Lentz, B. R. (1996) *Biochemistry 35*, 12602−12611.

Wu, J. R., & Lentz, B. R. (1994) *J. Fluoresc. 4*, 153−163.

BI9622332